Mitral valve asymmetry in healthy, pathological, and repaired cases

Cite as: Phys. Fluids **33**, 077118 (2021); https://doi.org/10.1063/5.0055485
Submitted: 29 April 2021 . Accepted: 17 June 2021 . Published Online: 20 July 2021

Dario Collia

Physics of Fluids ARTICLE scitation.org/journal/phf

Mitral valve asymmetry in healthy, pathological, and repaired cases

Cite as: Phys. Fluids **33**, 077118 (2021); doi: 10.1063/5.0055485
Submitted: 29 April 2021 · Accepted: 17 June 2021 ·
Published Online: 20 July 2021 · Publisher error corrected: 21 July 2021

Dario Collia[a)]

AFFILIATIONS

Department of Engineering and Architecture, University of Trieste, Trieste, Italy

[a)]Author to whom correspondence should be addressed: dar.collia@gmail.com

ABSTRACT

The entry of blood into the left ventricle is regulated by the two valve leaflets. Mitral valve prolapse is the primary cause of mitral regurgitation. Mitral valve repair is the gold standard therapeutic procedure for patients with degenerative mitral valve regurgitation and follows two fundamental principles: restoring a good coaptation surface of the flap and correcting annular dilation. This study presents a first step in the direction of addressing the influence of valve geometry on valve fluid dynamics and mitral regurgitation. To this end, it develops a systematic analysis to identify how the level of regurgitation and the efficiency of flow transit in the left ventricle depend on the degree of asymmetry of the leaflets. The analysis is performed starting from a mathematically designed mitral valve and then extended to the actual valves extracted from medical imaging. The specific objective is to evaluate the changes in mitral regurgitation associated with the symmetrical properties of the mitral valve. The broader aim is to begin building physics-based means for evaluating repair options and prosthetic design. Results showed that valve shape does not affect flow; sub-volumes are similar to inflow and vary to outflow due to the presence of false regurgitation under healthy/repaired conditions and regurgitation under pathological conditions affecting the amount of direct flow, delayed and finally the Stroke volume. The best valve asymmetry point was found to be 0.25, while the optimal range was between 0.4 and 0.2, giving an important suggestion to valve surgery.

I. INTRODUCTION

The mitral valve (MV) is constituted of an approximately circular annulus and two leaflets attached to it. The two leaflets feature a marked asymmetry: the anterior leaflet attaches to two fifths of the annular circumference, has a semicircular shape, and is about twice longer than the posterior one, which has a quadrangular shape attached to approximately three fifths of the annular circumference.[1] Mitral valve prolapse (MVP) is a common MV pathology that affects approximately the 2.4% of population. MVP is due to an insufficient closure of the two leaflets during systole that does not allow the MV to fulfill the task of preventing backflow. MVP represents the first cause of mitral regurgitation (MR),[2] the development of blood flow across the valve back to the left atrium during ventricular contraction. In chronic degenerative MR, both the left ventricle (LV) and the left atrium are subjected to an increase in load,[3] which causes an adaptive remodeling of both the left ventricular and atrial components that induce an increase in their size over time.[4] On the other hand, late systolic volume is reduced and afterload can be low, but as the ventricle enlarges and adapts to chronic volume overload, the afterload gradually increases.[5]

During the years, different methods have been developed to treat this pathology. The first option was the substitution with a mechanical or biological prosthetic valve; this, however, brings along several complications.[6,7] To date, the recommended treatment for degenerative mitral valve disease is mitral valve repair (MVR), as opposed to valve replacement with a biological or mechanical valve, because surgical valve reconstruction is associated with improved event-free survival.[8–10] Surgical MVR is the gold standard therapeutic procedure for patients with degenerative mitral valve regurgitation[8,11] and follows two fundamental principles: restore a good surface of leaflet coaptation and correct for annular dilatation.[8,12,13] Transcatheter solutions represent additional options that are currently recommended only in patients at risk.[9,10,14] Despite the reparation is the gold standard, endovascular replacement is expected to increase with the improvement and availability of endovascular prosthesis.

The relevance of blood flow regurgitation is typically evaluated by the effective regurgitant orifice area (EROA);[15–17] a structural measure given by the size of the valvular opening when it should be in closed position (during systole). Although EROA is the main measure

of valvular insufficiency, it does not completely define how much the valve is predisposed to regurgitation. Indeed, the fluid dynamics about the valve also depends on the geometry of the MV[18] and different valves with the same EROA can produce different amount of regurgitation. In this respect, valvular symmetry can be hypothesized to play a key role, while the MV natural asymmetry can be altered during a disease or be modified by the therapeutic choice. However, the understanding of the role of MV asymmetric geometry to MR is still largely incomplete. The geometric properties are not accounted in the evaluation of MV performances or in the design of repair procedures, other than seeking analogy to a native shape.

This study presents a first step in the direction of addressing the influence of MV geometry to the fluid dynamics about the valve and MR. To this aim, it develops a systematic analysis to identify how the level of regurgitation and the efficiency of flow transit in the LV depends on the degree of asymmetry in the leaflets. The analysis is performed starting with a mathematically designed MV to allow full control of the geometric parameters and ensure a methodical ground. The analysis is then extended to real valves extracted from medical imaging including valves before and after surgical repair.

The specific aim is to evaluate the alterations of MR associated with MV symmetric properties. The wider objective is that of start building physics-based means to evaluate repair options and prosthesis design.

II. MATERIALS AND METHODS

A. Geometries

In this study, a total of 118 different MV geometries were evaluated by numerical simulations embedded in a normal left ventricle (LV). The geometry of the normal LV was obtained by 3D multilayer cardiovascular magnetic resonance (CMR) by combining three long axis edges corresponding to the two-, three-, and four-chamber projections as described above.[19] The entire LV endocardial surface is described by its 3D coordinates evaluated by interpolation on a structured mesh made of 768 points along the circumference and 384 points from the base to the apex; however, the results were independent of the specific number of interpolation points. LV geometry during all phases of the heartbeat is described by the position vector $\boldsymbol{X}(\vartheta, s, t)$ of its endocardial surface, where the structured parametric coordinates (ϑ, s) run along the circumference and from base to apex, respectively, and t is time. The position vector marks the points of the LV material, and their velocity is obtained from temporal differentiation.

The LV functional parameters are as follows: End Diastolic Volume (EDV) = 114 ml, End Systolic Volume (ESV) = 47 ml, Stroke volume = 67 ml, and Ejection Fraction (EF) = 59%. The LV and its volume curve are shown in Fig. 1.

The geometry of the MV, which is the central for this study, was obtained in two different modalities. In a first phase, an ideal MV model is used with a mathematical description introduced in a previous study.[20] The radius of the valve, $R = 1.1$ cm, is maintained constant to fit in the LV geometry with normal elliptic shape (a parameter describing the ratio between the leaflets length in the two perpendicular direction fixed to the value $\frac{1}{3}$). The asymmetry of this valve is described by a dimensionless parameter ε that describes the difference in length between the anterior and the posterior leaflets, normalized to the their sum.[20] The asymmetry was modified starting from an

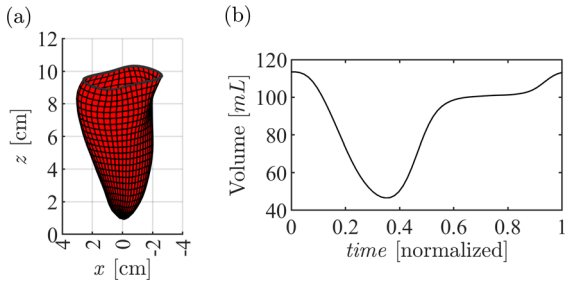

FIG. 1. LV geometry (a) and its volume curve (b).

extreme value $\varepsilon = 0.6$ to the value $\varepsilon = -0.6$ where the lengths of the anterior and posterior leaflet are $(1+\varepsilon)R$ and $(1-\varepsilon)R$, respectively. The analysis varies with continuously selecting 25 intermediate position with increments $\Delta\varepsilon = 0.05$. An example of these geometries in three different asymmetry configurations is shown in Figs. 2(a)–2(c).

The valve in the various position of opening is described parametrically by the degree of opening of each of the two leaflets, φ_1 and φ_2, for the anterior and posterior leaflets, respectively, that range from zero (closed leaflet) to $\frac{\pi}{2}$ (full open). Therefore, the valve is mathematically described by its coordinates $\boldsymbol{X}_v(\vartheta, s, \varphi_1, \varphi_2)$, where s range from zero at the annulus to 1 and the trailing edge ϑ is the azimuthal angle. The parameters φ_1 and φ_2 are the two degree of freedom describing the opening/closing dynamics ruled by equations that are described in Sec. II B.[15]

The same mathematical valve was used to reproduce MV with regurgitation [Figs. 2(d)–2(f)]. To this aim, the valve did not seal perfectly during closure because the leaflets were allowed to move a little backward (toward the atrium). They were considered three degrees of MR corresponding to $EROA = 0.26\,\text{cm}^2$, $EROA = 0.39\,\text{cm}^2$, and $EROA = 0.52\,\text{cm}^2$, respectively, for mild, moderate, and severe.[21–25] For each of them, the same modulation of asymmetry was analyzed, for a total of 25×3 simulations.

In a second phase, two real pathological MV geometries were recorded from 4D—transesophageal echocardiography, one with P2 type prolapse and one with P3 type prolapse. MV geometry was extracted from the images with the use of a dedicated software (4D MV-Assessment, TomTec Imaging Systems GmbH, Unterschleissheim, Germany) limitedly to the fully open (at peak diastole) and fully closed (peak systole) positions because the temporal resolution of current imaging technology is not sufficient to reliably visualize MV geometry during its rapid movement.

The extracted MV geometries were reorganized for convenience in terms of another pair of parametric coordinates (ϑ, s), which run along the circumference and extend, respectively, from the ring to the trailing edge and then be scaled in order to have the same annular size as the numerical valves.

The intermediate geometric configurations were reconstructed considering the two leaflets that moving independent of each other and each one associated with a degree of opening, say $\varphi_1(t)$ and $\varphi_2(t)$, for the anterior and posterior leaflets, respectively.

The same mathematical description given by $\boldsymbol{X}_v(\vartheta, s, \varphi_1, \varphi_2)$ represents a two-dimensional set of intermediate positions associated with the different degrees of leaflets' openings. These are estimated by a continuous modulation of the geometry from the closed

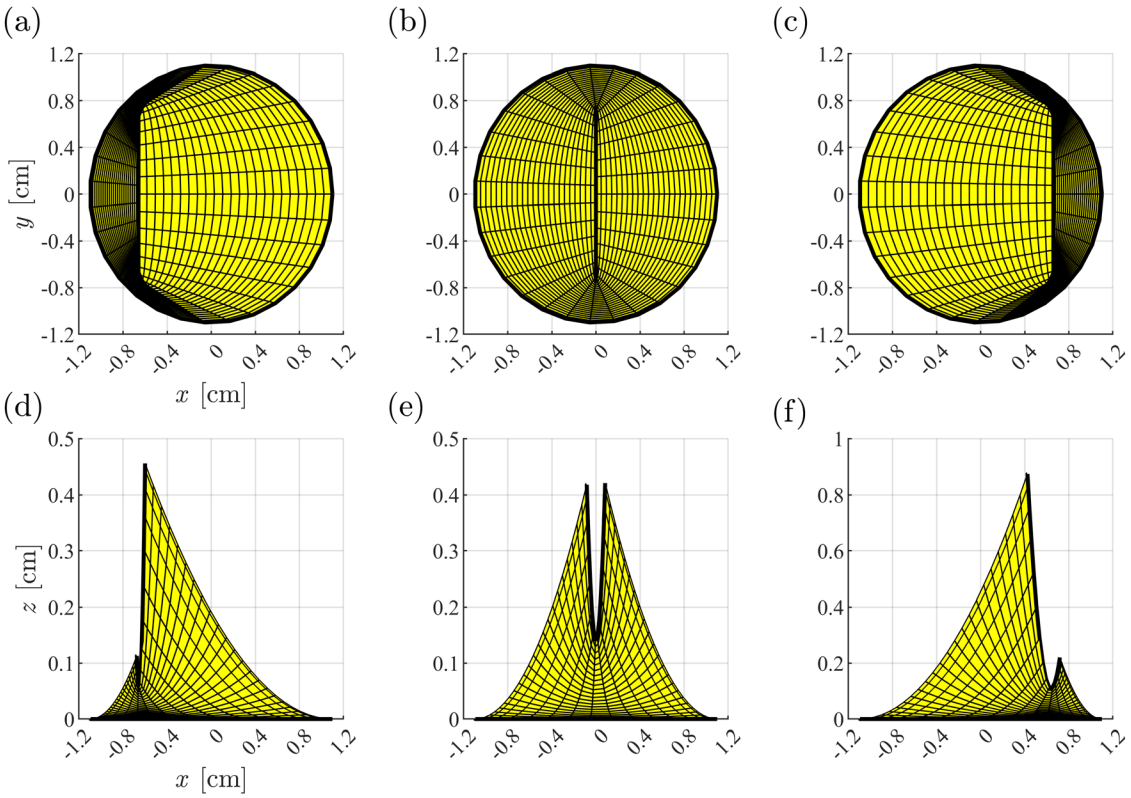

FIG. 2. Ideal valve in closed configuration for healthy (a)–(c) and insufficient (d)–(f) cases with asymmetry equal to (a) $\varepsilon = 0.6$, (b) $\varepsilon = 0$, and (c) $\varepsilon = -0.6$, respectively.

$X_v(\vartheta, s, 0, 0)$ to the open $X_v\left(\vartheta, s, \frac{\pi}{2}, \frac{\pi}{2}\right)$ recorded configurations as previously described.[15]

Then, the MV models are fit in the mitral position of the LV geometry. Furthermore, to evaluate the intermediate conditions of asymmetry, it is changed the size of the MV leaflets by moving the two edges from a position of more positive asymmetry to a value equal to $\varepsilon = 0.25$.

To evaluate the real MV at the same conditions of the ideal pathological valve, it is artificially modified the size of the prolapses through the lengthening of the leaflets to bring the frontal edges closer, thus obtaining an $EROA = 0.39\,\text{cm}^2$ for the P3 valve and an $EROA = 0.52\,\text{cm}^2$ for the P2 valve. This modification did not excessively offset the original values of the valves being already very close to the parameters of the ideal ones.

Figure 3 shows the real pathological valves with original [(a) and (c)] and modified [(b) and (d)] asymmetry. In order not to deform the valve, they have been obtained negative asymmetries simply by turning the valve; this allowed to carry out evaluations by expanding the number of prolapses thus obtaining cases with A1 and A2 prolapse. Therefore, in total were obtained six cases with positive asymmetry (P2–P3) and six with negative asymmetry (A1–A2) for a total of 12 analyzed cases.

The same method was adopted for a repaired valve obtaining six cases with three positive and three negative asymmetries. Both for the real pathological MV and for the repaired one, three types of asymmetries were chosen, one closer to the value $\varepsilon = 0.6$ ($\varepsilon = -0.6$), one closer to the value $\varepsilon = 0.4$ ($\varepsilon = -0.4$), and one closer to the value $\varepsilon = 0.25$ ($\varepsilon = -0.25$). An example in original configuration and one with modified asymmetry is shown in Fig. 4.

B. Fluid dynamics

The numerical method was extensively described and validated in a dedicated methodological study,[26] where the valvular dynamics was compared with another obtained by a complete fluid–structure interaction.[27] In this section, we briefly recall the main points of the method used. The intraventricular fluid dynamics is evaluated by numerical solution of the Navier–Stokes and continuity equations

$$\frac{\partial \boldsymbol{v}}{\partial t} + \boldsymbol{v} \cdot \nabla \boldsymbol{v} = -\nabla p + \nu \nabla^2 \boldsymbol{v}, \tag{1}$$

$$\nabla \cdot \boldsymbol{v} = 0, \tag{2}$$

where $\boldsymbol{v}(t, \boldsymbol{x})$ is the velocity vector field, $p(t, \boldsymbol{x})$ is the kinematic pressure field, and ν is the kinematic viscosity (assumed $0.04\,\text{cm}^2/\text{s}$). Blood is intentionally assumed as a Newtonian fluid. Indeed, blood is a mixture of elastic corpuscular elements in an aqueous solution and either Newtonian or non-Newtonian models are approximate. However, the influence of corpuscular or non-Newtonian behavior is

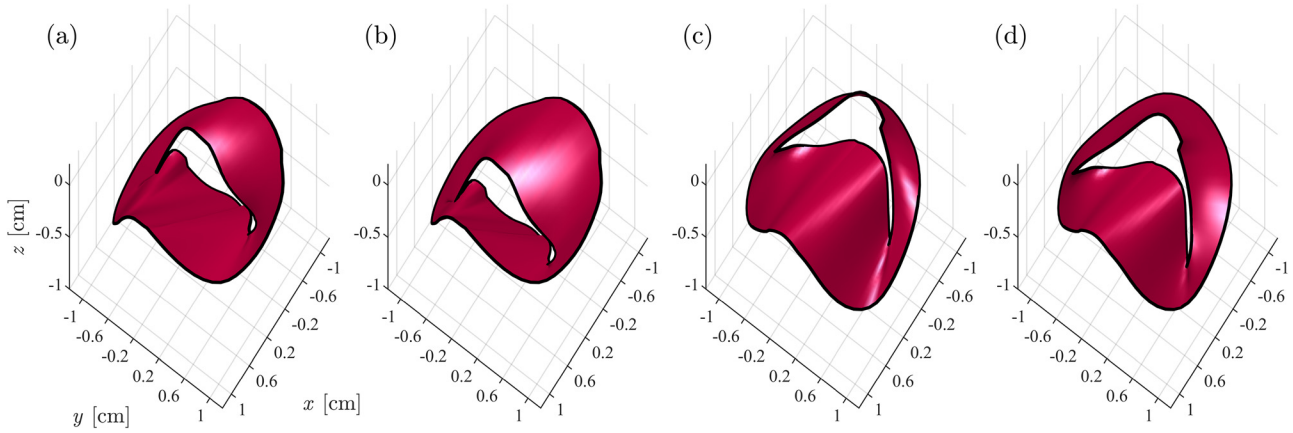

FIG. 3. Real pathological valve with P3 prolapse in original condition (a) and with modified asymmetry (b), and with P2 prolapse in original condition (c), and with modified asymmetry (d).

very small in the heart chambers[27] and it is negligible when compared with the limited accuracy of the clinical data used as input. Solution is achieved by the immersed boundary method in a bi-periodic Cartesian domain as described in previous studies, for example, Refs. 26 and 28–31. Time advancement is achieved using a fractional step method as follows. Velocity is preliminarily advanced in time by the Navier–Stokes equation [Eq. (1)] using a low-storage, third-order Runge–Kutta explicit scheme.

This preliminary velocity, $\hat{\boldsymbol{v}}$, that does not satisfy the incompressibility constraint (2), is corrected by adding a potential field $\delta\boldsymbol{v} = \nabla q$, such that $\boldsymbol{v} = \hat{\boldsymbol{v}} + \delta\boldsymbol{v}$ satisfies the continuity and the boundary conditions. The correction potential is found by solution of the Poisson equation

$$\nabla^2 \mathrm{q} = -\nabla \cdot \hat{\boldsymbol{v}}; \tag{3}$$

and pressure is updated with q accordingly. Boundary conditions at the edge of the computational box are set periodic in the x and y directions, while they are zero pressure and normal velocity on the upper and lower ends along with z, respectively. The 2D Fourier decomposition permits fast solution of the Poisson equation (3) as a sequence of tridiagonal systems for each harmonic. Boundary conditions are set on the moving immersed boundaries that comprise the ventricle geometry and valves surface. The boundary conditions are imposed on the intermediate velocity $\hat{\boldsymbol{v}}$ at the end of the Runge–Kutta time advancement before imposing the correction obtained by (3).[28] Given that the immersed boundaries do not coincide with the computational grid, a local interpolation scheme is commonly used to transfer the precise boundary conditions at the surrounding computational points.[27,32] In the present model, accounting that the physiological geometries present details not resolved in the imaging technology, that the used geometry represents only one realization within a range of natural variability, and that the boundary is mathematically represented as a surface of zero thickness, we have simplified the interpolation scheme by closing the cell containing the immersed boundary setting a speed equal to the average of the points falling into that cell. Furthermore, when calculating the Navier–Stokes equation at the closed cells corresponding to the soft tissues, the viscosity is artificially increased to its maximum stable value thus avoiding unrealistic sharp edge boundaries and improving numerical convergence. This implication of this simplification was evaluated in a previous study for the LV.[26] The overall numerical implementation was extensively validated in previous studies. In this study, it was used a bi-periodic domain with a grid made $128 \times 128 \times 160$ points and 8192 time steps.

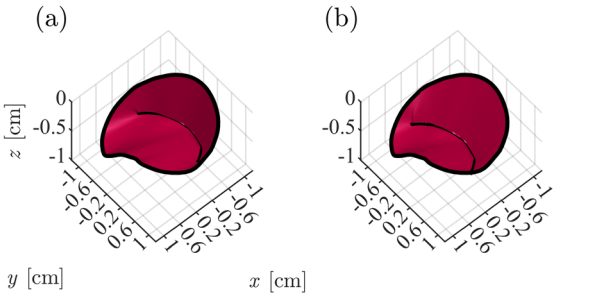

FIG. 4. Mitral valve repaired in original configuration (a) and with modified asymmetry (b).

Once the parametric description $\boldsymbol{X}_{\boldsymbol{v}}(\vartheta, s, \varphi_1, \varphi_2)$ is available, the dynamics equation of the leaflet-opening angle is obtained by the constraint that the motion of the leaflet surface must match the velocity of the fluid at the position of the same surface; a brief description is given below. A comprehensive description and verification of the computational method, including comparison with a fluid–structure interaction model with a given set of tissue parameters, are reported elsewhere.[26] The valvular leaflets are assumed to move with the flow with no elastic resistance other than the constraint of remaining in the set of configurations described by the two degrees of freedom. Under this assumption, the leaflet dynamics is obtained by least squares minimization of the difference, integrated over the valvular surface A_v, between the fluid and the valve velocity component normal to the valvular surface. The result is a 2×2 linear system,

$$\begin{bmatrix} \iint_{A_v}\left(\frac{\partial X_v}{\partial \varphi_1}\cdot n\right)^2 dA & \iint_{A_v}\left(\frac{\partial X_v}{\partial \varphi_1}\cdot n\right)\left(\frac{\partial X_v}{\partial \varphi_2}\cdot n\right)dA \\ \iint_{A_v}\left(\frac{\partial X_v}{\partial \varphi_1}\cdot n\right)\left(\frac{\partial X_v}{\partial \varphi_2}\cdot n\right)dA & \iint_{A_v}\left(\frac{\partial X_v}{\partial \varphi_2}\cdot n\right)^2 dA \end{bmatrix} \times \begin{bmatrix} \frac{\partial \varphi_1}{\partial t} \\ \frac{\partial \varphi_2}{\partial t} \end{bmatrix} = \begin{bmatrix} \iint_{A_v}(v\cdot n)\left(\frac{\partial X_v}{\partial \varphi_1}\cdot n\right)dA \\ \iint_{A_v}(v\cdot n)\left(\frac{\partial X_v}{\partial \varphi_2}\cdot n\right)dA \end{bmatrix}, \tag{4}$$

for the two unknowns $\frac{\partial \varphi_1}{\partial t}$ and $\frac{\partial \varphi_2}{\partial t}$, where v is the fluid velocity and n the local normal to valvular surface.

The dynamic model described by system (4) represents an asymptotic limit of the loosest MV within the prescribed set of geometric configurations. As the model reproduces an asymptotic behavior, it does not require the introduction of mechanical parameters of the tissues that would be otherwise necessary for solving the momentum equation for the solid. This is an advantage for applications where such properties are not available. This model represents an approximation with respect to a complete calculation with fluid–structure interaction, and it is not aimed to analyze the details of MV deformation. On the other hand, it has the advantage of not requiring a detailed definition of tissue properties that cannot be measured *in vivo*. This simplifies the solution that is aimed to reproduce the main properties of the LV fluid dynamics in the presence of a moving MV, assumed to have loose moving elements, when the general properties of the valvular structure are not available. A systematic analysis of the properties and limitations of such a valvular modeling for flow simulation is reported in a dedicated methodological study.[26] The aortic valve, which is, respectively, downstream of the LV flow field, is modeled as a simple orifice with a surface that opens when the MV is closed, and the average normal velocity at the valve position is directed toward the aorta and is closed in diastole.

C. Regurgitation

In this section, it is described the methods used for calculating MR properties. The effective orifice area of the MV orifice (MVO) area is computed by measuring the space between the leaflets trailing edge

$$MVO(t) = \int_0^L \left|X_{e_{ant}} - X_{e_{post}}\right| dL, \tag{5}$$

where $X_e = X_v(\vartheta, 1)$ is the trailing edge that is subdivided in the anterior and posterior leaflets, and L is the length of a curve running along the midpoint between the two edges. The EROA of a regurgitant orifice is the MVO evaluated from [Eq. (5)] during systole when the MV is in the closed configuration.

The calculation of the blood flow rate effectively crossing the MVO is computed by

$$Q_{MV}(t) = \int_0^L v_{rel}\cdot n\left|X_{e_{ant}} - X_{e_{post}}\right| dL, \tag{6}$$

where the relative velocity, $v_{rel} = \overline{v} - \frac{\partial}{\partial t}\frac{X_{e_{ant}} - X_{e_{post}}}{2}$, is the difference between the fluid velocity averaged along the line between the two facing edges and the velocity of the edges themselves, and n is the local normal. From this, the regurgitating blood volume is the flow crossing the MVO during systole

$$V_{reg} = \int_{sys} Q_{MV}(t)dt. \tag{7}$$

D. Flow transit

The evaluation of the flow transit is an important step for the identification of blood transport and mixing inside the LV in order to verify the blood residence and wash-out properties that are related to the risk of the thrombus formation. Following the established literature in cardiology,[34–37] this evaluation is obtained by subdividing the EDV into four sub-volumes

$$\mathrm{EDV} = V_{direct} + V_{delayed} + V_{retained} + V_{redisual}, \tag{8}$$

where V_{direct} is the volume of blood that entered during diastole and transits directly to the aortic outlet during systole, thus residing less than one heartbeat in the LV. $V_{retained}$ is the amount of blood volume that enters during diastole and is retained in the ventricle to be expelled on the next heartbeat. $V_{delayed}$ is the quantity of blood already present in the LV at the beginning of diastole and ejected during the following systole. Finally, $V_{residual}$ was present in the LV before the beginning of diastole and remains in the chamber after the end of systole.

These sub-volumes are defined through blood transport analysis that is performed by solving the transport-diffusion equation for a passive scalar

$$\frac{\partial C}{\partial t} + \nabla\cdot(vC) = \nu\nabla^2 C, \tag{9}$$

where $C(x,t)$ is the concentration of a passive marker of particles. Equation (9) is solved in parallel to the Navier–Stokes equation [Eq. (1)] starting from the initial condition $C(x,0) = 1$ at the beginning of diastole. Therefore, the average concentration starts from a unitary value and decreases progressively every heartbeat when the marked particles are replaces by fresh blood entered from the atrium. This method also allows differentiating the composition of fresh and old blood that enters and exits the LV and that regurgitates in the atrium.[38] The $V_{residual}$ is obtained with Eq. (9) from the evaluation as the following end systole

$$V_{residual} = \int_{ESV} C dV. \tag{10}$$

The volume of old blood regurgitated from the MV orifice is obtained by extending Eq. (6) as

$$Q_{MV_{old}}(t) = \int_0^L v_{rel}\cdot n\left|X_{e_{ant}} - X_{e_{post}}\right| C\, dL, \tag{11}$$

where C is the concentration measured at the MV orifice; the corresponding volume is

$$V_{reg_{old}} = \int_{sys} Q_{MV_{old}}(t)\, dt. \tag{12}$$

Through the difference between V_{reg} and $V_{reg_{old}}$, the quantity of fresh blood regurgitated in the atrium called $V_{reg_{new}}$ is obtained.

The outflow takes also into account the amount of regurgitated blood, which is the V_{reg}, so the SV becomes

$$\mathrm{SV} = V_{direct} + V_{delayed} + V_{reg}, \tag{13}$$

where V_{reg} is the total regurgitation composed of fresh and old blood.

Since the V_{direct} is the amount of fresh blood that enters and exits during the same beat, also the regurgitated part of blood will also be fresh and therefore

$$V_{direct_{outflow}} = V_{direct_{inflow}} - V_{reg_{new}}. \tag{14}$$

The same reasoning is made for the $V_{delayed}$, and it is associated with the $V_{reg_{old}}$ being blood already present in the previous beat and expelled in the current and therefore

$$V_{delayed_{outflow}} = V_{delayed_{inflow}} - V_{reg_{old}}. \tag{15}$$

Finally, the SV at the end of the outflow will change its original value if there is an amount of regurgitated blood, and then, its effective value is

$$SV_{eff} = \mathrm{SV} - V_{reg}. \tag{16}$$

III. RESULTS

A. Analysis with ideal healthy valve

A total of 25 cases were analyzed with healthy ideal valve by applying different asymmetry values from a negative to a positive direction (from $\varepsilon = -0.6$ to $\varepsilon = 0.6$ with step of 0.05).

At inflow, the shape of the valve does not influence the transit of blood. In fact, as shown in Fig. 5, the sub-volumes maintain a very similar value to each other despite the different valve asymmetry that determines their shape. At the beginning of diastole, more precisely at the value of ESV, the two sub-volumes $V_{residual}$ and $V_{delayed}$ are already present in the ventricle, at the same time the other two sub-volumes V_{direct} and $V_{retained}$ enter inside the ventricle until reaching the maximum value, which is EDV [Eq. (8)]. During the systole, the V_{direct} is expelled immediately with the $V_{delayed}$, while the remaining fresh blood is retained ($V_{retained}$) inside the ventricle; this value added to the $V_{residual}$ is equal to the ESV. These values are compatible with those existing in the literature.[36,39–42]

In Fig. 6 shows the flow direction in four cases, two extremes with $\varepsilon = 0.6$ and $\varepsilon = -0.6$ [Figs. 6(a) and 6(d)] and two with $\varepsilon = 0.25$ and $\varepsilon = -0.25$ [Figs. 6(b) and 6(c)], a full video is shown as multimedia view. A very positive asymmetry highlights the predominance of the posterior leaflet with a very deviating flow toward the posterior wall, as we approach a more balanced direction between the two leaflets the flow takes a more regular and physiological direction.[26,27,33,38,43] Negative asymmetry reverses the flow direction and makes the valve behave as if it were reversed.

Despite the different shapes of the valves, the transit of the flow does not vary; in fact, as can be seen in Figs. 6(e)–6(h) the distribution of the sub-volumes remains similar. At the apex of the ventricle, there is in all cases a dense red part representing the $V_{residual}$, the empty sections is the V_{direct}, which is directed toward the aorta and ready to be expelled, the mixed parts ($V_{retained}$ and $V_{delayed}$) are represented by a more transparent red where one part will be held and the other expelled. Analyzing these distributions in detail, it can therefore be said that in inflow the sub-volumes are similar whatever is the shape of the MV. As described in Sec. II D, another volume comes into play during the outflow, which is the V_{reg}. This value is also present in healthy valves as there is a part of blood (called false regurgitation), which is pushed into the atrium by the two leaflets of the MV during the closure phase before systole.[38] The regurgitated part of blood is made up of fresh and old blood, and the fresh part ($V_{reg_{new}}$) comes from V_{direct}, while the old part ($V_{reg_{old}}$) comes from $V_{delayed}$. Figure 7 shows how regurgitation affects the transit of blood from inflow to outflow. As previously mentioned there are two quantities of fresh blood that enter, one that comes out immediately and one that mixes with the blood already present in the ventricle, and in Fig. 7(a), it can be seen that not all the fresh blood comes out into the aorta during the systolic phase, but some part is pushed into the atrium during the closure of the leaflets.

This quantity, which is the $V_{reg_{new}}$, increases as the asymmetry moves toward a negative configuration [Fig. 7(c)], affecting the final value of V_{direct} at the outflow. The same goes for the $V_{delayed}$ [Fig. 7(b)], and it is reduced in a quantity of blood already present in the ventricle

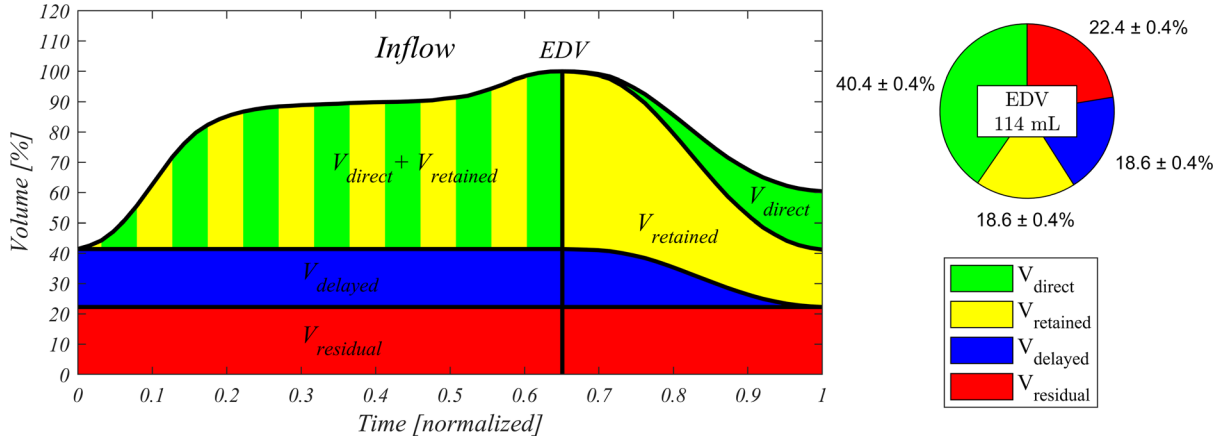

FIG. 5. The left side of the graph shows the average trend of the sub-volumes, while the right side shows the pie graph of sub-volumes in percentage of EDV and with their uncertainty.

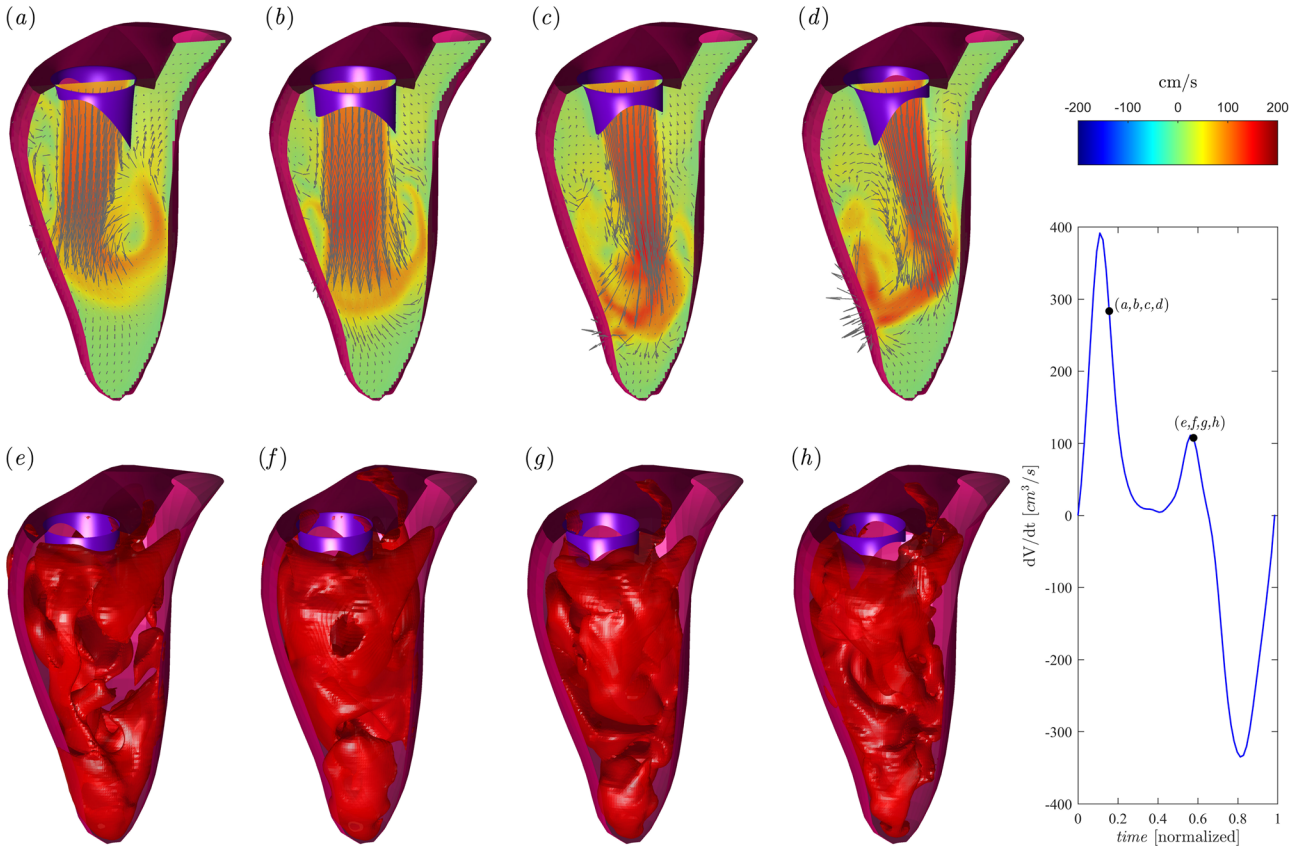

FIG. 6. Fluid velocity field of ideal healthy valves with (a) $\varepsilon = 0.6$, (b) $\varepsilon = 0.25$, (c) $\varepsilon = -0.25$, and (d) $\varepsilon = -0.6$ as indicated in the box of the volume curve; the speed module is indicated by the color from red to blue from -200 units to 200 units (cm/s). Three-dimensional flow field calculated with the passive scalar iso-surface method at the same instants of late diastole in the first heartbeat at value C = 0.4 with (e) $\varepsilon = 0.6$, (f) $\varepsilon = 0.25$, (g) $\varepsilon = -0.25$, and (h) $\varepsilon = -0.6$ as indicated in the box of the volume curve. Multimedia view: https://doi.org/10.1063/5.0055485.1 of fluid velocity field [(a)–(d)].

from the previous beat, which is $V_{reg_{old}}$ [Fig. 7(c)] and is pushed into the atrium together with the $V_{reg_{new}}$. These amounts of old and new blood, shown in Fig. 7(c), show how they grow as valve asymmetry increases, and in particular, we note that asymmetries where regurgitation is minimal or almost zero are between 0.2 and 0.4. This is an important fact, which is also reflected in the evaluation of all sub-volumes, as it indicates that an excellent valve asymmetry is in that range.

Regurgitation therefore also influences the SV, and in fact, in Fig. 7(d) it can be seen how it varies from the inflow (which is always the same) to the outflow generating a new effective SV value as the valve asymmetry varies with an excellent valve asymmetry in the range identified above.

To confirm what has been said, Fig. 8 shows how regurgitation actually influences the transit of these sub-volumes. The two pie graphs show a substantial difference between MV with positive and negative asymmetry, and in fact, a valve with a more positive asymmetry regurgitates a total amount of blood equal to 1.1% [Fig. 8(a)], and this quantity is reduced with asymmetry [Fig. 8(b)]. The same evaluation with a negative asymmetric valve shows how regurgitation effectively increases [Fig. 8(c)] up to the most extreme case that is 5.4% [Fig. 8(d)].

These differences of regurgitated blood for different asymmetry values can be given by the different length of the leaflets and by a greater proximity toward the left ventricular outflow tract (LVOT) for negative asymmetries and greater proximity to the posterior wall of the ventricle for positive asymmetries.

Starting from the case of the valve with negative asymmetry, this phenomenon can be explained as follows: during early systole, the blood is pushed with great speed toward the aorta; a part of this blood is channeled into the valve finding an opening and therefore returning to the atrium; this process ends almost immediately as the leaflets are closing, but the amount of regurgitated blood is greater than in a valve with positive asymmetry precisely because it is located near the LVOT; and the length of the leaflets also affects the quantity of blood transported to the atrium, which in fact varies from 2.3% to 5.4%, respectively, for $\varepsilon = 0$ and $\varepsilon = -0.6$.

On the other hand, in cases with positive asymmetry the valve behaves differently. Starting from the extreme case ($\varepsilon = 0.6$) the regurgitation is equal to 1.1%, this value is due to the proximity of the closing point of the two leaflets with the posterior wall, which is already in the phase of systolic contraction [as can be seen from the direction regurgitation in Fig. 8(a)] and the length of the posterior leaflet. This regurgitation value is reduced until it reaches a minimum at

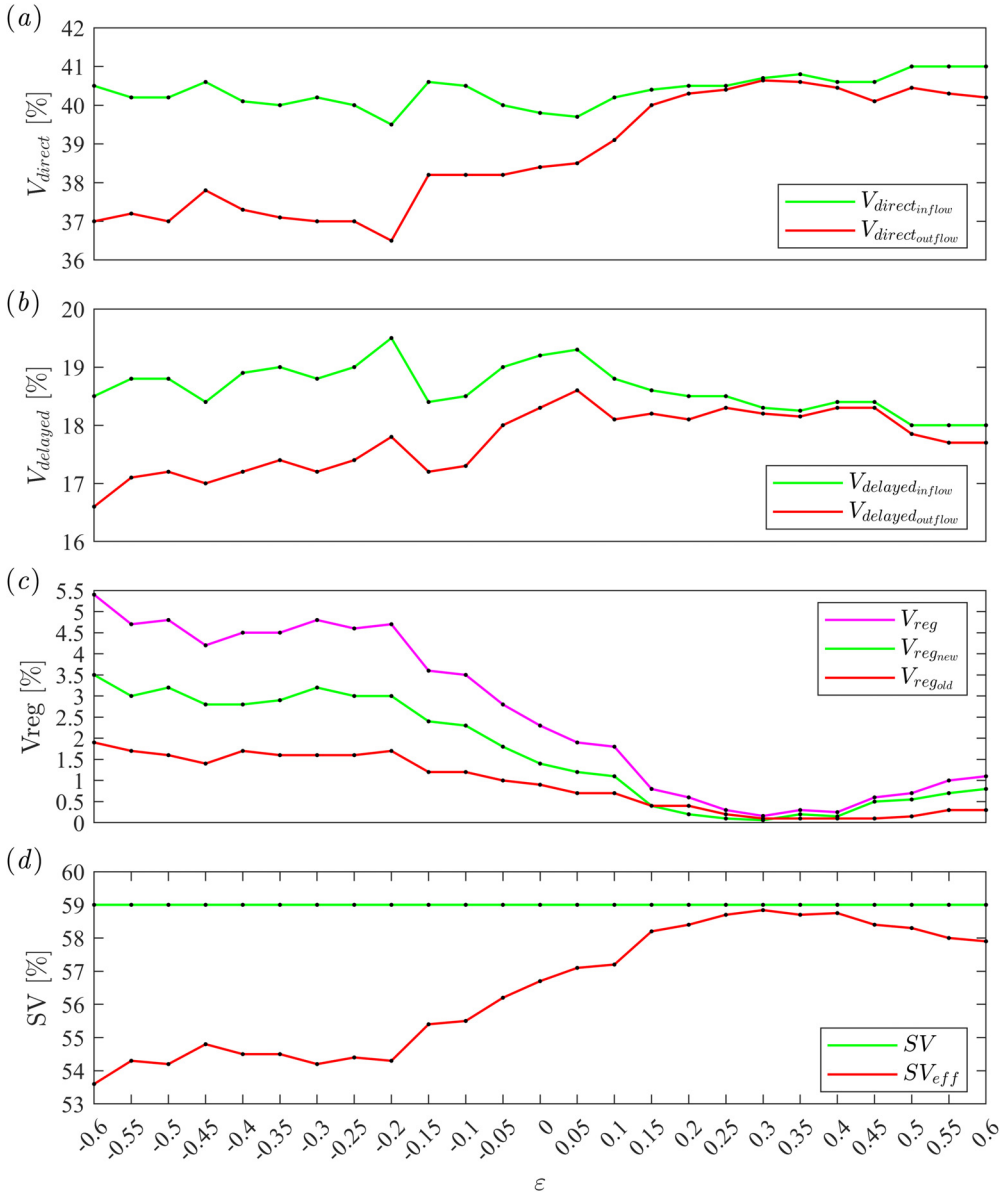

FIG. 7. Trend of the sub-volumes, regurgitation, and SV as the valve asymmetry varies at the inflow and outflow. (a) V_{direct}, (b) $V_{delayed}$, (c) V_{reg}, and (d) SV.

$\varepsilon = 0.3$; from here on, it gradually grows back to the maximum point of asymmetry $\varepsilon = -0.6$. That said, we can define a physiological asymmetry range that is between $\varepsilon = 0.4$ and $\varepsilon = 0.2$ with an optimal value of $\varepsilon = 0.25$. This value is defined optimum taking in consideration the composition of fresh and old regurgitated blood [as showed in Fig. 7(c)], and in fact, a minor quantity of old blood regurgitated reducing considerably the probability of thrombus formation.

B. Analysis with ideal insufficient valve

The same analysis was done by adapting the ideal valve to the pathological conditions to verify how the quantity of regurgitated blood changes as the asymmetry varies even in these conditions. To obtain these conditions, the direction of the ideal valve flaps toward the atrium was forced, simulating the pathological condition of the MR, while the asymmetry varies with the regurgitation orifice equal to: $EROA = 0.26\,\text{cm}^2$, $EROA = 0.39\,\text{cm}^2$, and $EROA = 0.52\,\text{cm}^2$ for a total of 75 cases.

In Fig. 9, the distribution of inflow sub-volumes of all pathological cases is shown, which is equal to healthy cases.

At the outflow, however, the regurgitation comes into play and as in the previous case it affects the V_{direct} and the $V_{delayed}$ influencing the valve with more negative asymmetry than the more positive one.

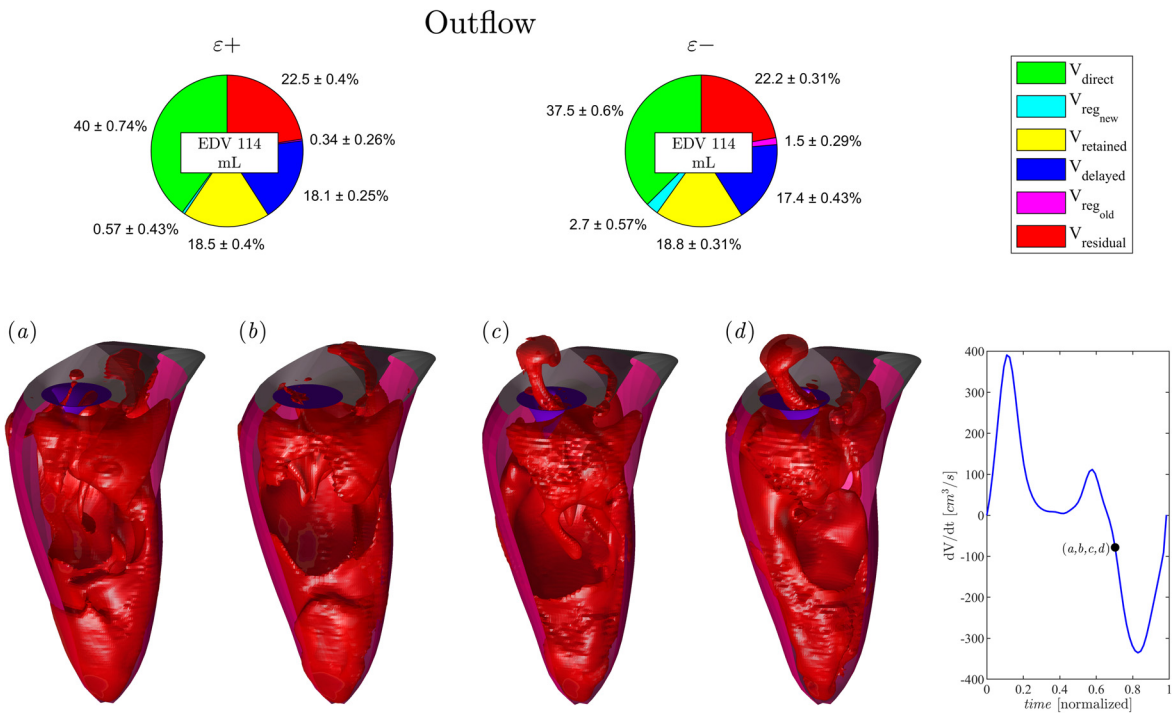

FIG. 8. In the upper section, the mean with their standard deviation of the sub-volumes in cases of MV with negative and positive asymmetric form is shown. In the lower section, it is shown the three-dimensional flow field calculated with the passive scalar iso-surface method at the same instants of early systole in the first heartbeat at value C = 0.35 with (a) $\varepsilon = 0.6$, (b) $\varepsilon = 0.25$, (c) $\varepsilon = -0.25$, and (d) $\varepsilon = -0.6$ as indicated in the box of the volume curve.

As is known, valve regurgitation is correlated with EROA,[38] but as can be seen in Table I it also varies depending on the valve asymmetry. The amount of blood expelled into the atrium substantially modifies the quality and quantity of the sub-volumes as well as the SV_{eff}, which varies considerably in the case of more severe regurgitation making a healthy ventricle behave as an extremely pathological one. In order to validate this, thesis was made simulations using two real pathological valves but with the modified asymmetry thus obtaining cases with a prolapse of type P2 and P3 and an $EROA = 0.52\,\text{cm}^2$, respectively, for valves with positive asymmetry and A2 and A1 with an $EROA = 0.39\,\text{cm}^2$ for negative asymmetry. This allows having a more complete evaluation for different cases with characteristics similar to the ideal ones having the same *EROA* and the same valve radius.

In the upper section of Fig. 10, it is shown a pie chart with the distribution of the sub-volumes at the inflow and outflow of these pathological valves. As can be seen, also in this case, the transit of blood to the inflow behaves as in a healthy condition. At the outflow, however, the blood transit follows always the same pattern, namely, that the quantity of regurgitated blood is influenced by the valve asymmetry. In fact in the points [(a)–(d)] of Fig. 7, it is possible to see how the quantity of regurgitated blood varies depends on the shape of the valve. A detail of these values extended for all cases is shown in Table II.

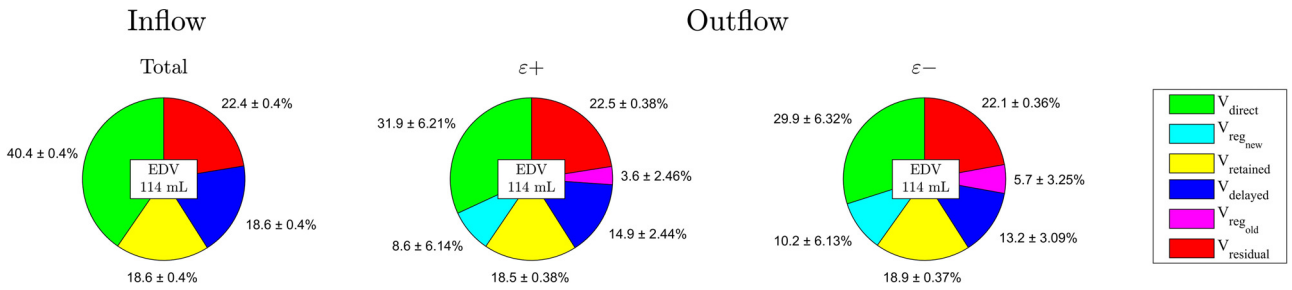

FIG. 9. The pie graph shows the distribution of the sub-volumes at the inflow (mean ± SD) of all pathological cases and the subdivision at the outflow for the cases with positive and negative asymmetry.

TABLE I. Values of the sub-volumes at the outflow of the ideal pathological valves at the two extreme points of asymmetry ($\varepsilon = -0.6$ and $\varepsilon = 0.6$) and at the ideal point ($\varepsilon = 0.25$) with its negative antagonist ($\varepsilon = -0.25$).

Case (ε)	EROA (cm^2)	V_{direct} (%)	$V_{residual}$ (%)	$V_{delayed}$ (%)	$V_{retained}$ (%)	V_{reg} (%)	$V_{reg_{new}}$ (%)	$V_{reg_{old}}$ (%)	SV_{eff} (%)
−0.6	0.26	34.8	22.6	15	18.4	9.2	5.8	3.4	49.8
−0.25	0.26	35.7	21.6	17.3	19.4	6	3.9	2.1	53
0.25	0.26	39.2	22.5	17.8	18.5	2	1.3	0.7	57
0.6	0.26	36.4	23	16.1	18	6.5	4.6	1.9	52.5
−0.6	0.39	30.5	22.4	12.3	18.6	16.2	9.9	6.3	42.8
−0.25	0.39	32.2	21.7	14	19.3	12.8	7.5	5.3	46.2
0.25	0.39	34.1	22.2	15.6	18.8	9.3	6.1	3.2	49.7
0.6	0.39	31	22.7	13.8	18.3	14.2	9.7	4.5	44.8
−0.6	0.52	20.4	21.7	8.1	19.3	30.5	19.3	11.2	28.5
−0.25	0.52	22.4	21.9	9.6	19.1	27	17.5	9.5	32
0.25	0.52	24.1	22.2	11.8	18.8	23.1	16.1	7	35.9
0.6	0.52	21	22.3	9.5	18.7	28.5	19.3	9.2	30.5

In fact, the valves with the prolapse of the posterior leaflet regurgitate a smaller quantity of old blood, improving the $V_{residual}$ by a value equal to 2%. This is shown in Fig. 10(a) where it can be seen that the blood is well mixed, while in (b) there is a quantity of fresh blood at the apex of the ventricle. In the case of negative asymmetry, this value remains fairly constant, the $V_{delayed}$ is considerably reduced, and the quantity of old blood is greater. This can be seen in Figs. 10(c) and 10(d) where there is a predominance of old blood in the distribution within the ventricle.

C. Analysis with real repaired valve

Mitral valve repair is the gold standard used in the case of severe valve disease.[1,8,11,44] In this and other types of repairs, it is not clear

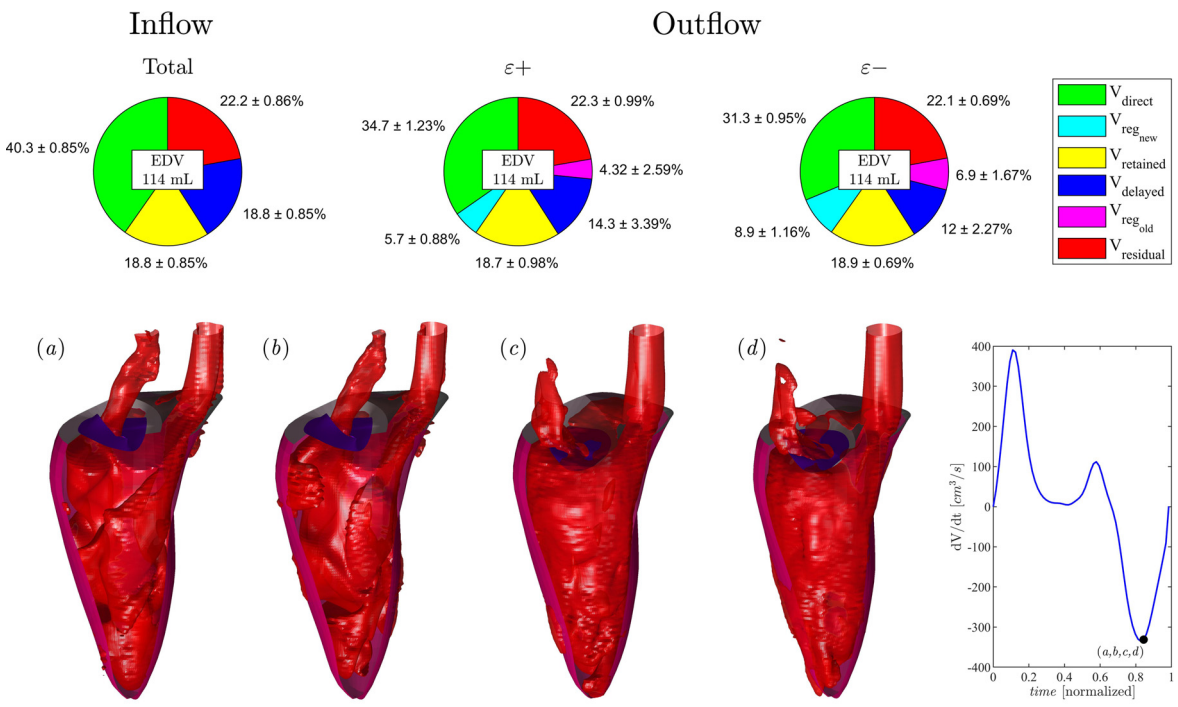

FIG. 10. In the upper section, the mean with their standard deviation of the sub-volumes at the inflow and outflow in cases of real pathological MV with negative and positive asymmetric form is shown. In the lower section, it is shown the three-dimensional flow field calculated with the passive scalar iso-surface method at the same instants at middle of systole in the first heartbeat at value C = 0.35 with (a) $\varepsilon = 0.6$, (b) $\varepsilon = 0.25$, (c) $\varepsilon = -0.25$, and (d) $\varepsilon = -0.6$ as indicated in the box of the volume curve.

TABLE II. Values of the sub-volumes at the outflow of the real pathological valves.

Case (ε)	$EROA$ (cm^2)	V_{direct} (%)	$V_{residual}$ (%)	$V_{delayed}$ (%)	$V_{retained}$ (%)	V_{reg} (%)	$V_{reg_{new}}$ (%)	$V_{reg_{old}}$ (%)	SV_{eff} (%)
A1 (−0.6)	0.39	30	21.8	12.9	19.2	16.1	9.8	6.3	42.9
A1 (−0.4)	0.39	30.7	21.6	13.8	19.4	14.5	8.9	5.6	44.5
A1 (−0.25)	0.39	31.5	21.8	14.35	19.15	13.2	8.4	4.8	45.8
P3 (0.25)	0.39	33.2	20.8	18.35	20.15	7.5	5.7	1.8	51.5
P3 (0.4)	0.39	33.4	21.6	17.5	19.4	8.1	6.2	1.9	50.9
P3 (0.6)	0.39	33.9	22.6	16.55	18.35	8.6	6.8	1.8	50.4
A2 (−0.6)	0.52	30.8	23.6	7.4	17.4	20.8	10.8	10	38.2
A2 (−0.4)	0.52	31.7	21.7	11.6	19.3	15.7	8	7.7	43.3
A2 (−0.25)	0.52	33	22.3	11.8	18.7	14.2	7.3	6.9	44.8
P2 (0.25)	0.52	36.2	22.7	12.8	18.3	10	4.5	5.5	49
P2 (0.4)	0.52	35.8	22.3	11.9	18.7	11.3	4.5	6.8	47.7
P2 (0.6)	0.52	35.7	24	8.9	17	14.4	6.3	8.1	44.6

what is the ideal final position of the leaflets that determines an ideal valve asymmetry. In this regard, numerical simulations were made with a repaired valve whose valve asymmetry was changed in one direction or another.

In the upper section of Fig. 11, it shows the distribution of the sub-volumes in inflow and outflow. In inflow, the flow passes regularly and the distribution is linear and in accordance with the healthy and pathological cases previously described. In outflow, we can see how the valve, although well repaired, shows an almost absent false regurgitation in the configuration with positive asymmetry and a greater false regurgitation in the configuration with negative asymmetry.

Table III shows how the values of the sub-volumes are influenced due to the valve asymmetry; false regurgitation increases more in negative asymmetry to be four times larger than in a repair with positive one. The concentration of old and new blood inside the ventricle is strongly influenced by the valvular asymmetry; a valve repaired with asymmetry $\varepsilon = 0.25$ [Fig. 11(b)] regurgitates a minimal quantity of

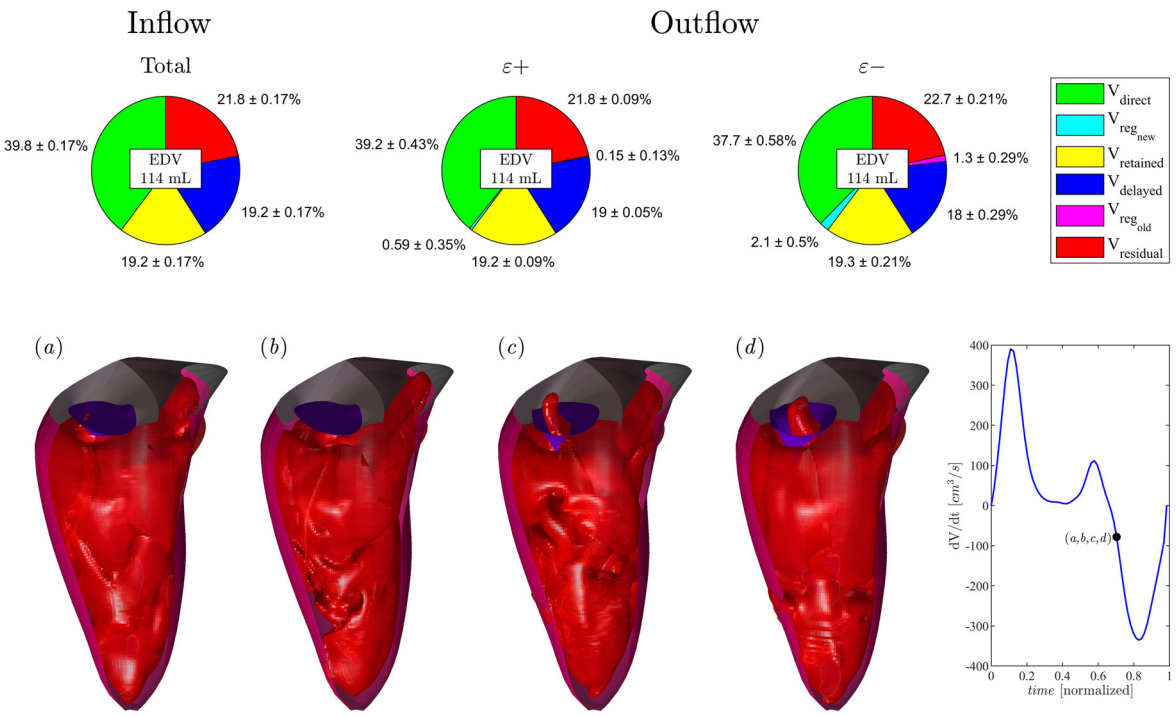

FIG. 11. In the upper section, the mean with their standard deviation of the sub-volumes at the inflow and outflow in cases of repaired MV with negative and positive asymmetric form is shown. In the lower section, it is shown the three-dimensional flow field calculated with the passive scalar iso-surface method at the same instants of early systole in the first heartbeat at value C = 0.35 with (a) $\varepsilon = 0.6$, (b) $\varepsilon = 0.25$, (c) $\varepsilon = -0.25$, (d) $\varepsilon = -0.6$ as indicated in the box of the volume curve.

TABLE III. Values of the sub-volumes at the outflow of the real repaired valves.

Case (ε)	V_{direct} (%)	$V_{residual}$ (%)	$V_{delayed}$ (%)	$V_{retained}$ (%)	V_{reg} (%)	$V_{reg_{new}}$ (%)	$V_{reg_{old}}$ (%)	SV_{eff} (%)
MVR (−0.6)	36.9	21.5	17.9	19.5	4.2	2.6	1.6	54.8
MVR (−0.4)	37.8	22	17.7	19	3.5	2.2	1.3	55.5
MVR (−0.25)	38.3	21.7	18.4	19.3	2.3	1.4	0.9	56.7
MVR (0.25)	39.76	21.9	19	19.1	0.15	0.14	0.01	58.85
MVR (0.4)	39.25	21.9	19	19.1	0.75	0.65	0.1	58.25
MVR (0.6)	38.71	21.7	18.97	19.3	1.32	0.99	0.33	57.68

fresh and almost no old blood with a good distribution within the ventricle. The same cannot be said in the case of negative asymmetry $\varepsilon = -0.6$ [Fig. 11(d)] where the valve regurgitates a significant quantity of blood, to be a repaired valve, influencing the distribution of ventricular blood with a greater distribution of old blood at the apex of LV.

IV. DISCUSSIONS

Valvular asymmetry is a parameter that effectively influences significantly the distribution of sub-volumes and the quantity of blood regurgitated into the atrium. The results showed that a MV with more negative asymmetry regurgitates a greater amount of blood than the

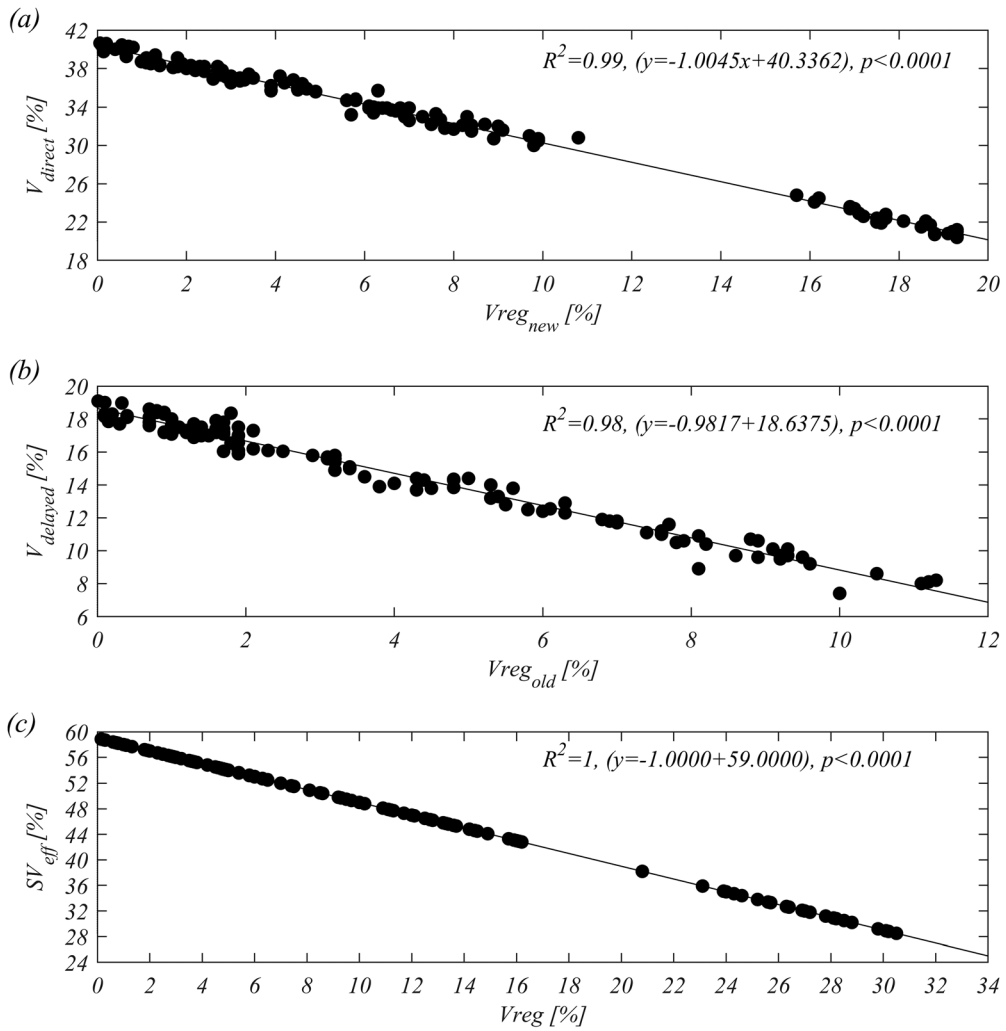

FIG. 12. Correlation between (a) V_{direct} and $V_{reg_{new}}$, (b) $V_{delayed}$ and $V_{reg_{old}}$, and (c) SV_{eff} and V_{reg}.

opposite cases; this happens because the closure point of the two leaflets is in the direction closest to the LVOT and with the anterior leaflet longer respect the posterior. In cases with healthy ideal MV, the presence of false regurgitation followed this phenomenon, which was subsequently extended to all the other cases analyzed. In the global evaluation of the regurgitated blood volumes, it is therefore important the evaluation of the old and new blood quantity; a regurgitated quantity of fresh blood is immediately reintroduced into the circulation at the next heartbeat, while a quantity of old blood continues to flow between the atrium and ventricle with each beat, risking creating thrombus over time. The results showed that the least amount of regurgitated blood is given by the asymmetry value $\varepsilon = 0.3$ even if this amount is mostly old blood. From what has been said before, it is also important to evaluate the combination between fresh and old blood, and in this regard, the ideal value was found to be $\varepsilon = 0.25$ as it regurgitates a minimum quantity of old and mostly fresh blood. This is important and is a great step toward a broader evaluation of valve repair and the design of various types of valve prostheses. Therefore, the optimal valve asymmetry interval is between $\varepsilon = 0.4$ and $\varepsilon = 0.2$ with the optimal point centered at $\varepsilon = 0.25$.

The shape of the valve does not affect the inflow of the valve where the sub-volumes are practically the same, but it predominates on the evaluation of the outflow that is strongly influenced by the values of the regurgitated blood, as well as by the SV. To confirm the data, in Fig. 12 it shows the correlations between the sub-volumes take in examination; in label (a), there is a strong correlation ($R^2 = 0.99$) between V_{direct} and $V_{reg_{new}}$ ($p < 0.0001$), in label (b) between $V_{delayed}$ and $V_{reg_{old}}$ ($R^2 = 0.98$) ($p < 0.0001$), and in the label (c) between SV_{eff} and V_{reg} ($R^2 = 1$) ($p < 0.0001$). The null hypothesis was rejected for $P < 0.05$.

The purpose of this work is not only evaluative but above all to give a point of reference to MV cardiac surgery; for example, during an MVR it is important to orient the two leaflets in the optimal point of asymmetry to minimize the presence of false regurgitation and improve the flow transit of the blood, as seen in Sec. III C. These indications allow the cardiac surgeon to optimize the surgical technique on a large scale, significantly affecting the survival rate. Another inspiration is given on the design of valve prostheses, these results indicating how a correct choice of valve asymmetry considerably increases the success of a good prosthesis. A correct valvular asymmetry allows obtaining a correct directionality of the flow inside the ventricle, useful for avoiding pathological onset such as cardiomyopathies of various types and onset of mitral and aortic pathologies.

ACKNOWLEDGMENTS

The author acknowledges partial support by Italian Ministry of Education and Research under Project No. PRIN 2017 A889FP.

DATA AVAILABILITY

The data that support the findings of this study are available from the corresponding author upon reasonable request.

REFERENCES

[1]D. H. Adams, A. C. Anyanwu, P. B. Rahmanian, and F. Filsoufi, "Current concepts in mitral valve repair for degenerative disease," Heart Fail. Rev. **11**, 241–257 (2006).
[2]L. A. Freed, D. Levy, R. A. Levine, M. G. Larson, J. C. Evans, D. L. Fuller, B. Lehman, and E. J. Benjamin, "Prevalence and clinical outcome of mitral-valve prolapse," New Engl. J. Med. **341**, 1–7 (1999).
[3]B. Ren, L. E. de Groot-de Laat, and M. L. Geleijnse, "Left atrial function in patients with mitral valve regurgitation," Am. J. Physiol. **307**(10), H1430–1437 (2014).
[4]M. Cameli, E. Incampo, and S. Mondillo, "Left atrial deformation: Useful index for early detection of cardiac damage in chronic mitral regurgitation," IJC Heart Vasculature **17**, 17–22 (2017).
[5]W. H. Gaasch and T. E. Meyer, "Left ventricular response to mitral regurgitation," Circulation **118**, 2298 (2008).
[6]Y. Shapira, M. Vaturi, and A. Sagie, "Hemolysis associated with prosthetic heart valves: A review," Cardiol. Rev. **17**, 121–124 (2009).
[7]D. K. C. Cooper and R. Wagner, "Xenotransplantation," Nonhuman Primates in Biomedical Research **1**, 391–402 (2012).
[8]D. H. Adams, R. Rosenhek, and V. Falk, "Degenerative mitral valve regurgitation: Best practice revolution," Eur. Heart J. **31**, 1958–1966 (2010).
[9]A. Colli, D. Adams, A. Fiocco, N. Pradegan, L. Longinotti, M. Nadali, D. Pandis, and G. Gerosa, "Transapical NeoChord mitral valve repair," Ann. Cardiothorac. Surg. **7**, 812–820 (2018).
[10]M. Ali Elbey, L. A. Palma Dalan, and G. Ferragut Attizzani, "Value of MitraClip in reducing functional mitral regurgitation," US Cardiol. Rev. **13**(1), 30 (2019).
[11]J. G. Castillo, A. C. Anyanwu, V. Fuster, and D. H. Adams, "A near 100% repair rate for mitral valve prolapse is achievable in a reference center: Implications for future guidelines," J. Thorac. Cardiovasc. Surg. **144**(2), 308–312 (2012).
[12]A. Carpentier, "Cardiac valve surgery-the 'French correction'," J. Thorac. Cardiovasc. Surg. **86**(3), 323–337 (1983).
[13]E. Braunberger, A. Deloche, A. Berrebi, F. Abdallah, J. A. Celestin, P. Meimoun, G. Chatellier, S. Chauvaud, J. N. Fabiani, and A. Carpentier, "Very long-term results (more than 20 years) of valve repair with Carpentier's techniques in nonrheumatic mitral valve insufficiency," Circulation **104**, 8–11 (2001).
[14]G. W. Stone, J. A. Lindenfeld, W. T. Abraham, S. Kar, D. S. Lim, J. M. Mishell, B. Whisenant, P. A. Grayburn, M. Rinaldi, S. R. Kapadia, V. Rajagopal, I. J. Sarembock, A. Brieke, S. O. Marx, D. J. Cohen, and N. J. Weissman, "Transcatheter mitral-valve repair in patients with heart failure," N. Engl. J. Med. **379**(24), 2307–2318 (2018).
[15]D. Collia, L. Zovatto, and G. Pedrizzetti, "Analysis of mitral valve regurgitation by computational fluid dynamics," APL Bioeng. **3**, 036105 (2019).
[16]M. Enriquez-Sarano, J. B. Seward, K. R. Bailey, and A. J. Tajik, "Effective regurgitant orifice area: A noninvasive Doppler development of an old hemodynamic concept," J. Am. Coll. Cardiol. **23**(2), 443–451 (1994).
[17]W. L. Henry, J. M. Griffith, L. L. Michaelis, C. L. McIntosh, A. G. Morrow, and S. E. Epstein, "Measurement of mitral orifice area in patients with mitral valve disease by real-time, two-dimensional echocardiography," Circulation **51**(5), 827–831 (1975).
[18]V. Delgado, L. F. Tops, J. D. Schuijf, A. de Roos, J. Brugada, M. J. Schalij, J. D. Thomas, and J. J. Bax, "Assessment of mitral valve anatomy and geometry with multislice computed tomography," JACC Cardiovasc Imaging **2**(5), 556–565 (2009).
[19]G. Pedrizzetti, P. M. Arvidsson, J. Töger, R. Borgquist, F. Domenichini, H. Arheden, and E. Heiberg, "On estimating intraventricular hemodynamic forces from endocardial dynamics: A comparative study with 4D flow MRI," J. Biomech. **60**, 203 (2017).
[20]F. Domenichini and G. Pedrizzetti, "Asymptotic Model of Fluid—Tissue Interaction for Mitral Valve Dynamics," Cardiovasc. Eng. Technol. **6**(2), 95–104 (2015).
[21]E. Ashikhmina, D. Shook, F. Cobey, B. Bollen, J. Fox, X. Liu, A. Worthington, P. Song, and S. Shernan, "Three-dimensional versus two-dimensional echocardiographic assessment of functional mitral regurgitation proximal isovelocity surface area," Anesth. Analg. **120**, 534 (2015).
[22]A. Smer, N. C. Nanda, R. E. Akdogan, Z. M. Elmarzouky, and S. Dulal, "Echocardiographic evaluation of mitral valve regurgitation," Mini-Invasive Surg. **4**, 52 (2020).
[23]P. G. Chew, K. Bounford, S. Plein, D. Schlosshan, and J. P. Greenwood, "Multimodality imaging for the quantitative assessment of mitral regurgitation," Quant. Imaging Med. Surg. **8**, 342 (2018).

[24]P. Lancellotti, C. Tribouilloy, A. Hagendorff, B. A. Popescu, T. Edvardsen, L. A. Pierard, L. Badano, J. L. Zamorano, O. Bruder, B. Cosyns, E. Donal, R. Dulgheru, M. Galderisi, D. Muraru, K. Nieman, R. Sicari, D. reviewers, K. Haugaa, G. L. Canna, J. Magne, and E. Plonska, "Recommendations for the echocardiographic assessment of native valvular regurgitation: An executive summary from the European Association of Cardiovascular Imaging," Eur Heart J Cardiovasc Imaging. **14**(7), 611–644 (2013).
[25]E. Apostolidou, A. D. Maslow, and A. Poppascorresponding, "Primary mitral valve regurgitation: Update and review," Glob Cardiol Sci Pract. **2017**(1), e201703.
[26]D. Collia, M. Vukicevic, V. Meschini, L. Zovatto, and G. Pedrizzetti, "Simplified mitral valve modeling for prospective clinical application of left ventricular fluid dynamics," J. Comput. Phys. **398**, 108895 (2019).
[27]V. Meschini, M. D. De Tullio, G. Querzoli, and R. Verzicco, "Flow structure in healthy and pathological left ventricles with natural and prosthetic mitral valves," J. Fluid Mech. **834**, 271–307 (2018).
[28]F. Domenichini, "On the consistency of the direct forcing method in the fractional step solution of the Navier-Stokes equations," J. Comput. Phys. **227**(12), 6372–6384 (2008).
[29]J. O. Mangual, F. Domenichini, and G. Pedrizzetti, "Describing the highly three dimensional right ventricle flow," Ann. Biomed. Eng. **40**(8), 1790–1801 (2012).
[30]J. O. Mangual, E. Kraigher-Krainer, A. De Luca, L. Toncelli, A. Shah, S. Solomon, G. Galanti, F. Domenichini, and G. Pedrizzetti, "Comparative numerical study on left ventricular fluid dynamics after dilated cardiomyopathy," J. Biomech. **46**(10), 1611–1617 (2013).
[31]F. Domenichini and G. Pedrizzetti, "Hemodynamic forces in a model left ventricle," Phys. Rev. Fluids **1**, 083201 (2016).
[32]R. Mittal, H. Dong, M. Bozkurttas, F. M. Najjar, A. Vargas, and A. von Loebbecke, "A versatile sharp interface immersed boundary method for incompressible flows with complex boundaries," J. Comput. Phys. **227**, 4825 (2008).
[33]D. Collia, L. Zovatto, G. Tonti, and G. Pedrizzetti, "Comparative Analysis of Right Ventricle Fluid Dynamics," Front. Bioeng. Biotechnol. **9**, 667408 (2021).
[34]A. F. Bolger, E. Heiberg, M. Karlsson, L. Wigström, J. Engvall, A. Sigfridsson, T. Ebbers, J. P. E. Kvitting, C. J. Carlhäll, and B. Wranne, "Transit of blood flow through the human left ventricle mapped by cardiovascular magnetic resonance," J. Cardiovasc. Magn. Reson. **9**(5), 741–747 (2007).
[35]C. J. Carlhäll and A. Bolger, "Passing strange: flow in the failing ventricle," Circulation **3**(2), 326–331 (2010).
[36]V. M. Stoll, A. T. Hess, C. T. Rodgers, M. M. Bissell, P. Dyverfeldt, T. Ebbers, S. G. Myerson, C.-J. Carlhäll, and S. Neubauer, "Left Ventricular Flow Analysis," Circulation **12**(5), e008130 (2019).
[37]G. Pedrizzetti and F. Domenichini, "Nature optimizes the swirling flow in the human left ventricle," Phys. Rev. Lett. **95**(10), 108101 (2005).
[38]D. Collia, L. Zovatto, and G. Pedrizzetti, "Analysis of mitral valve regurgitation by computational fluid dynamics," APL Bioeng. **3**(3), 036105 (2019).
[39]E. Svalbring, A. Fredriksson, J. Eriksson, P. Dyverfeldt, T. Ebbers, A. F. Bolger, J. Engvall, and C.-J. Carlhäll, "Altered diastolic flow patterns and kinetic energy in subtle left ventricular remodeling and dysfunction detected by 4D flow MRI," PLoS One **11**, e0161391 (2016).
[40]A. G. Fredriksson, J. Zajac, J. Eriksson, P. Dyverfeldt, A. F. Bolger, T. Ebbers, and C. J. Carlhäll, "4-D blood flow in the human right ventricle," Am. J. Physiol. **301**(6), H2344–H2350 (2011).
[41]J. Eriksson, A. F. Bolger, T. Ebbers, and C. J. Carlhäll, "Four-dimensional blood flow-specific markers of LV dysfunction in dilated cardiomyopathy," Eur. Heart J. Cardiovasc. Imaging. **14**(5), 417–424 (2013).
[42]H. Kaur, H. Assadi, S. Alabed, D. Cameron, V. S. Vassiliou, J. J. M. Westenberg, R. Van Der Geest, L. Zhong, A. Dastidar, A. J. Swift, P. Garg, S. A. Alabed, S. A. Uk, A. J. A. Swift, and A. J. S. Uk, "Left Ventricular Blood Flow Kinetic Energy Assessment by 4D Flow Cardiovascular Magnetic Resonance: A Systematic Review of the Clinical Relevance," J Cardiovasc Dev Dis. **7**(3), 37 (2020).
[43]J. H. Seo and R. Mittal, "Effect of diastolic flow patterns on the function of the left ventricle," Phys. Fluids **25**(1), 110801 (2013).
[44]M. Daimon, S. Fukuda, D. H. Adams, P. M. McCarthy, A. M. Gillinov, A. Carpentier, F. Filsoufi, V. M. Abascal, V. H. Rigolin, S. Salzberg, A. Huskin, M. Langenfeld, and T. Shiota, "Mitral valve repair with Carpentier-McCarthy-Adams IMR ETlogix annuloplasty ring for ischemic mitral regurgitation: early echocardiographic results from a multi-center study," Circulation **114**(1), 588–593 (2006).